

Z'_{B-L} phenomenology at LHC

Y. A. Coutinho

Instituto de Física–Universidade Federal do Rio de Janeiro
Av. Athos da Silveira Ramos 149
Rio de Janeiro - RJ, 21941-972, Brazil

E. C. F. S. Fortes, J. C. Montero

Instituto de Física Teórica–Universidade Estadual Paulista
R. Dr. Bento Teobaldo Ferraz 271
São Paulo - SP, 01140-070, Brazil

Abstract

We study the Z' phenomenology for two extensions of the Electroweak Standard Model (SM) which have an extra $U(1)_{B-L}$ gauge factor. We show the capabilities of the LHC in distinguishing the signals coming from these two extensions and both of them from the Standard Model background. In order to compare the behavior of these $B-L$ models we consider the reaction $p + p \longrightarrow \mu^+ + \mu^- + X$ and compute some observables as the total cross sections, number of events, forward-backward asymmetry, final particle distributions like rapidity, transverse momentum, and dimuon invariant mass, for two LHC regimes: $\sqrt{s}(\mathcal{L}) = 7$ TeV (1 fb^{-1}) and 14 TeV (100 fb^{-1}) for $M_{Z'} = 1000$ GeV and 1500 GeV. We show that by using appropriate kinematic cuts some of the observables considered here are able to extract different properties of the Z' boson, and hence providing information about to which $B-L$ model it belongs to.

PACS:14.70.Pw, 12.60.Cn, 12.15.Ji

elaine@ift.unesp.br; montero@ift.unesp.br; yara@if.ufrj.br

1 Introduction

The starting up of the Large Hadron Collider (LHC) operating in an energy range far above the electroweak scale, offers a possibility to reveal new phenomena and to explore the phenomenology extracted from the expected huge amount of experimental data. In this way, it is expected new physics manifestations throughout the appearance of new degrees of freedom such as new charged and neutral fermions, superpartners, new gauge bosons, and Higgs scalar(s). To take into account these new possible degrees of freedom we must go beyond the SM. There are many ways to construct extensions of the electroweak SM. However, if we are concerned with new gauge bosons we must consider a larger gauge group. Whatever the extension of the SM is, it must present the same results of the SM at the electroweak energy scale in order to be consistent with present data.

Although hadron colliders present a high background (pile-up) compared to electron-positron (beamstrahlung) colliders, they seem to be more suitable for discovering new degrees of freedom. Since high centre-of-mass energy and high precision can not be achieved simultaneously in the same experiment, both types of colliders are needed in order to have a detailed description of a particular phenomena. This is easily realized if we look to a recent past, when the synergy between hadron and lepton colliders, brought up complementary information for each other, generating benefits to high energy physics. As examples we have the discovery of the Z boson, the gluon, and the quark top. The discovery of the Z boson occurred in a $p\bar{p}$ collider (SPS) but its properties (decay widths, couplings to fermions, asymmetries, mass, etc...) were measured with high precision in lepton colliders (SLC, LEP). In this way, the recent studies started at LHC can direct the search for new physics in future linear colliders (ILC/CLIC).

Among the main goals of any accelerator proposal we find the physics of an extra neutral gauge boson Z' . This new boson is predicted by many extensions of the Standard Model like:

- The models from E_6 group, also know as rank 5 models (ER5M) [3, 4];
- The Left-Right which are based in the group $SU(2)_L \otimes SU(2)_R \otimes U(1)_{B-L}$ [5];
- The models with Z' in Little Higgs scenario [6];
- The Sequential Standard models - SSM [7];
- The Kaluza Klein (KK) models, predicted by extra dimensions [8];

- The models with $SU(3)_c \times SU(3)_L \times U(1)_N$ gauge symmetry, known as 3-3-1 models [9, 10, 11];
- Models where a strong dynamics is involved in the electroweak spontaneous symmetry breaking. We can cite, for instance, Topcolor and BESS (Breaking Electroweak Symmetry Strongly) models [12].

Some models which have an extra $U(1)$ gauge group [13, 14] also deserve a detailed study in order to predict new physics behavior. The cumulative study of different models, candidates to describe the electroweak interaction, can guide the LHC data analysis if in fact a Z' is discovered. The extra $U(1)$ group gives rise to the Z' vector boson. The new constraints on these models generate few free parameters, if we compare them to other models which have origin in larger gauge groups. Following the arguments here exposed, first we have considered the Z' boson observables for electron-positron colliders [15], and now we extend the study for hadron colliders.

In this paper, we study the phenomenology of the Z' boson originated from two different extensions of the electroweak SM with an extra $U(1)$ gauge factor. We predict the possible signals of new physics in the process $p+p \rightarrow (\gamma, Z, Z') \rightarrow \mu^+ + \mu^- + X$, at the tree level. We compare several quantities as total cross sections, number of events, and decay widths assuming that both $U(1)$ factors correspond to the local $B - L$ symmetry, and that the breaking of this symmetry occurs at an energy scale above the TeV scale.

In order to have a more realistic scenario, we choose the parameters and constraints of the two different models to compare them at the same Z' boson mass. We use $M_{Z'} = 1500$ GeV, but we also show the results for $M_{Z'} = 1000$ GeV, for two centre-of-mass energies: $\sqrt{s} = 7$ and 14 TeV.

This article is organized in the following way. In section II we introduce the models. In section III we present the results and in section IV we present our conclusions.

2 The models

In this paper we consider two extensions of the electroweak SM which have an extra $U(1)$ local factor, resulting in the total gauge symmetry $SU(2)_L \otimes U(1)_1 \otimes U(1)_2$. More specifically, we are concerned with models which are based on the gauge symmetries:

- $SU(2)_L \otimes U(1)_Y \otimes U(1)_z$, called as Secluded model [13];
- $SU(2)_L \otimes U(1)_{Y'} \otimes U(1)_{B-L}$ called as Flipped model [14].

In the Secluded model, z is a new $U(1)$ charge, and Y is the electroweak SM hypercharge. In the Flipped one, Y' is a new extra $U(1)$ charge, and the $B - L$ charge assignments are those of the SM. In this last model the SM hypercharge is recovered after the first spontaneous symmetry breaking. In the Secluded model, the electric charge has no component in the $U(1)_z$ and in particular, depending on the value of this charge, several versions of this model can be studied. Our analysis will be focused on comparing both models only when the z charge of the Secluded model coincides with $B - L$. Besides, in this minimal version, considered here, both models have the same scalar sector, composed by one doublet, H , with hypercharge $Y = +1$, and a complex singlet with $Y = 0$. The number of right-handed neutrinos is three, in order to be consistent with the anomaly cancellations. We had set them to be heavy enough in order to have Z' decay into heavy right-handed neutrinos kinematically suppressed. Besides that, the minimal version considered here is also absent of exotic decay channels like heavy quarks or heavy charged leptons. So, our results of decay widths, branchings fractions for these two particular Z' models are related only to standard model fermions. We will parameterize the neutral currents in terms of the mass eigenstate fields as follows:

$$\mathcal{L}^{NC} = -\frac{g}{2c_W} \sum_i \bar{\psi}_i \gamma_\mu [(g_V^i - g_A^i \gamma_5) Z_1^\mu + (f_V^i - f_A^i \gamma_5) Z_2^\mu] \psi_i. \quad (1)$$

In this paper we briefly present both models. The complete details about both of them were subject of study in a recent work [15]. Moreover, the scalar sector of this sort of models, with the respective Feynman rules, is considered in reference [16]. The charge operators for the Secluded and the Flipped models, are respectively given by:

$$\frac{Q}{e} = I_3 + \frac{1}{2} Y,$$

$$\frac{Q}{e} = I_3 + \frac{1}{2} [Y' + (B - L)].$$

When the z charge of the Secluded model is equal to $B - L$ it implies that the parameter z_H (the z -charge of the SM Higgs doublet), discussed in Refs. [13, 14], is equal to zero. In this case, there is no tree level mixing in the mass matrix between the neutral gauge bosons B_z^μ , W_3^μ and B_Y^μ , and we have $Z = Z_1$ and $Z' = Z_2$, i.e. the mass eigenstates and the symmetry eigenstates coincide. This is not the case for the Flipped model. Here, we

	<i>Neutrinos</i>	<i>Leptons</i>	<i>u – quarks</i>	<i>d – quarks</i>
f_V	0.8420	0.4977	−0.0511	−0.3955
f_A	−0.1732	0.1715	−0.1732	0.1732

Table 1: Z' coupling constants to the SM fermions for the Flipped model for $M_{Z'} = 1500$ GeV.

will assume that the mixing between the two neutral vector bosons is small enough so that $Z \approx Z_1$ and $Z' \approx Z_2$.

Both models are well motivated since, in general, they can be thought as an intermediate symmetry, remnant of a larger (unknown) gauge symmetry, that was broken at a very large energy scale. Moreover, they are simpler compared to other class of models with an extra Z' neutral vector boson: simpler gauge groups and fewer free parameters.

3 Results

We have first chosen $M_{Z'} = 1500$ GeV in order to compare the results coming from the two different models. For the Secluded model, this choice respects the bounds already established on the Z' boson mass and its coupling constants by the direct search at the Tevatron [17], by the electroweak precision tests (EWPT) at LEP II, and by the low-energy neutral current experiments [18, 19, 20], which are well studied in the literature. On the other hand, the Flipped model has not received the same level of attention. We find that it also deserves a detailed study to establish constraints on its parameters and numerical couplings.

For the Flipped model we use the following inputs: $g_{B-L} = 0.6132$, $g' = 0.4400$, $u = 1987$ GeV, $v = 246$ GeV, $\alpha = 127.9$, and $s_W^2 = 0.23122$ [21]. With these parameters we obtain $M_{Z'} = 1500$ GeV, $\Gamma_{Z'} = 28.39$ GeV, and the values of the neutral current coupling constants shown in Table 1. The Z couplings with SM fermions remain the same so we emphasize only the new contribution from the Z' boson.

For the Secluded model we use as inputs: $z_H = 0$, $g_z = 0.2$, $z_q = z_u = 1/3$, $u = 7500$ GeV, and $v = 246$ GeV. With these parameters we obtain $M_{Z'} = 1500$ GeV, $\Gamma_{Z'} = 4.04$ GeV, and the values of the neutral current coupling constants shown in Table 2. Due to the choice $z_H = 0$ in the Secluded model, the Z' boson has only vector couplings to fermions, and presents a *leptophilic*

	<i>Neutrinos</i>	<i>Leptons</i>	<i>u – quarks</i>	<i>d – quarks</i>
f_V	0.2690	0.2690	-0.0897	-0.0897
f_A	0	0	0	0

Table 2: Z' coupling constants to the SM fermions for the Secluded model for $M_{Z'} = 1500$ GeV.

$M_{Z'} = 1500$ GeV	Flipped $B - L$	Secluded $B - L$
$Z' \rightarrow \sum_i \bar{\nu}_i \nu_i$	36%	37.5%
$Z' \rightarrow \sum_i l_i \bar{l}_i$	18.6%	37.5%
$Z' \rightarrow \sum_i \bar{q}_i q_i$	42.6%	25%
$Z' \rightarrow W^+ W^-$	2.8%	0%

Table 3: The Z' partial decay widths for fermions and charged vector boson for both $B - L$ models.

behavior around the peak region. The *leptophilic* character means that the Z' boson couples preferentially to leptons, and that the cross section for lepton production presents a higher peak compared to quark cross sections. This behavior can be seen with more evidence in $e^+ + e^- \rightarrow l + \bar{l}$ process, where l is a lepton.

We can realize through the partial decay widths that, as we said before, for the Secluded model, Z' couples preferentially to leptons, as shown in Table 3. Due to this character, and depending on the choice of the Z' parameters, the Secluded model can give an explanation for the positron excess in cosmic rays, as presented by the PAMELA experiment [22].

We present in Figure 1 the total Z' decay width against $M_{Z'}$. Both of them are linear functions of $M_{Z'}$, as it should be, and hence they double their values in the Z' boson mass range showed in the figure. However, according to the parameter choice, $g_z = 0.2$, the decay width of the Secluded model is smaller than that of the Flipped one. In the latter model the Z' boson has both axial and vector couplings, and in the Secluded model it has only the vector ones due to the choice $z_H = 0$.

The Z' production can be achieved by the Drell-Yan mechanism which implies in leptonic decay products accompanied by background, which contaminates the observables under consideration. This background can be minimized applying some specific cuts. To perform our calculations we use the package Comphep [23] with Cteq6L1 parton distribution functions.

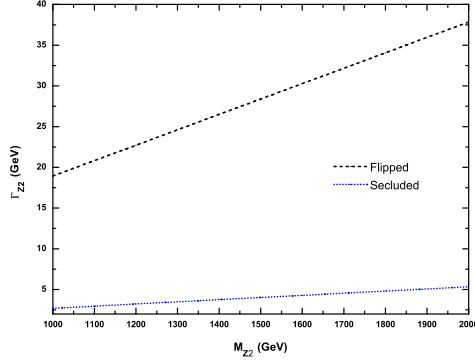


Figure 1: Evolution of total decay width with Z' boson mass.

For the first simulations we have used the following cuts on the final leptons, which we call as the first cut set: $p_{t\mu} > 20$ GeV, $|\eta_\mu| \leq 2.5$ and $-0.99 < \cos \theta_{q\mu} < 0.99$.

The first observable obtained, when the first cut set is used, is the total cross section for $p + p \rightarrow (\gamma, Z, Z') \rightarrow \mu^+ + \mu^- + X$. Considering $M_{Z'} = 1500$ GeV we obtain for the Flipped, Secluded and SM, 1.33×10^3 pb, 1.01×10^3 pb, and 0.6×10^3 pb, respectively for $\sqrt{s} = 14$ TeV, which implies considering the annual luminosity $\mathcal{L} = 100 \text{ fb}^{-1}$ in a huge number of events: $\sim 10^8$. We present in Table 4 the number of events considering $M_{Z'} = 1500$ and 1000 GeV for both models and also $\sqrt{s} = 14$ and 7 TeV. The number of events will decrease when we apply more restrictive cuts. In order to assign the correct quark direction, we had selected dimuon large rapidity events, $|y_{\mu\mu}| > 0.8$, as suggested in [24, 25], the other cuts are $p_{t\mu} > 20$ GeV, $|\eta_\mu| \leq 2.5$, $1450 \text{ GeV} < M_{\mu\mu} < 1550 \text{ GeV}$, and $-0.99 < \cos \theta_{q\mu} < 0.99$, and we call them as the second cut set.

Besides the total cross section and decay width for leptonic final state, we present: invariant mass, rapidity, forward-backward asymmetry, transverse momentum and angular distribution. In Figures 2a and 2b we present the dilepton invariant mass distribution. The Flipped model presents a distinct behavior with a higher peak far above the Standard model and has very good changes to be separated from the background. On the other, the Secluded model distribution in the region off-peak in Figure 2 (down panel) has a behavior similar to that of the SM, while the on-peak region is not

Model	$M_{Z'} = 1500$ GeV	$M_{Z'} = 1000$ GeV	$M_{Z'} = 1000$ GeV
Flipped $B - L$	1.33×10^8	8.48×10^3	245
Secluded $B - L$	1.01×10^8	7.18×10^3	219

Table 4: Number of events considering $M_{Z'} = 1500$ and 1000 GeV, and the first cut set. The second and third columns are for $\sqrt{s} = 14$ and $\mathcal{L} = 100fb^{-1}$, and the forth column is for $\sqrt{s} = 7$ TeV and $\mathcal{L} = 1fb^{-1}$. In the data related to $M_{Z'} = 1000$ GeV we have also set $M_{\mu\mu} > 500$ GeV.

so powerful to distinguish it from the SM. This difference has origin mainly in the choice of $z_H = 0$ for the Secluded model, which leads to pure vector couplings of the Z' boson to fermions. A different choice for z_H , say $z_H \neq 0$, will restore the axial couplings but, in this case, the z -charge will not be equal to $B - L$. The case of $z_H \neq 0$ is out of the scope of the present work. The rapidity distributions can also be used to disentangle the $B - L$ models. This observable is powerful even when we consider both light and heavy quarks or only the light ones, this result is showed in Figures 3a, 3b and 3c. The signal has been improved for both models but once again the Flipped model produces a signal above the ones of the other two models. One intrinsic characteristic of the Flipped model is the increasing signal until it reaches the region where the rapidity of each muon is $|y_\mu| = 1.25$. Both, the Secluded model and the SM do not have this behavior. When we apply more severe cuts on rapidity, as $|y_\mu| > 0.8$, the resulting data reveal that the three models have less possibilities to be disentangled. So, for this observable, the first cut set is more efficient than the more severe ones.

Another important observable, very sensitive to the new physics contributions, is the forward-backward asymmetry (A_{FB}^ℓ). In e^+e^- colliders, A_{FB}^ℓ is measured with high precision, due to the well known initial beam direction. However, the situation is quite different for hadron colliders where the original quark direction is completely unknown. To solve this problem, the quark direction can be approximated by the boost direction, which connects the dimuon reference system with the original beam direction. In order to achieve this goal we have applied the $|y_{\mu\mu}| > 0.8$ cut for the muon pair rapidity, following the references [24, 25]. In contrast with the Flipped model, the Secluded one has no Z' axial couplings to fermions and, as a consequence of it, the forward-backward asymmetry, even being a powerful tool to get information on the Z' boson parameters, does not receive contributions from the axial couplings on-peak. In the Figure 4 we show this observable versus $M_{\mu\mu}$, and we see that the two $B - L$ models can be distinguished.

If we consider all the studied observables, after applying the second cut set, we will realize that one particular numerical cut can put in evidence one observable and others not. The cut $|y_{\mu\mu}| > 0.8$ is not so helpful for rapidity distributions, but it is necessary for forward-backward asymmetries in order to guarantee that the quark direction has more probability to be the correct one. It means that the probability of obtaining more significant measurements of forward-backward asymmetries increases for higher rapidities.

We present in the Figure 5 our results for the muon transverse momentum distribution. One of the characteristics of this distribution is that the peak is located right at the position $p_T = M_{Z'}/2$, for both $B - L$ models. We have adopted more restricted cuts in the final dimuon mass, $M_{\mu\mu} > 500$ GeV [26] in order to emphasize this behavior. The flipped has once again, much better chances to be separated from the background, in opposition, the Secluded one can be mistaken as Standard model background.

The muon angular distribution is less sensitive to Z' contributions, but can be used as a previous result before the calculation of A_{FB}^ℓ . From Figure 6 we can realize that the signals related to the SM are below the signals of the two $B - L$ models. We can see a small asymmetry when the curves cross each other in the region $-0.50 < \cos\theta < -0.25$, where θ is the angle between the beam and the muon directions.

We now consider a Z' boson which mass is 1000 GeV and $\sqrt{s} = 7$ and 14 TeV in order to extract more conclusions about the same observables presented above. The related graphs are presented in the Figures 7, 8, 9 and 10. The increase of the centre of mass energy from 7 to 14 TeV has as direct consequences the increase of the cross sections and, hence, the number of events. The invariant mass distribution shows also a small peak for the Secluded model if compared to the Flipped one, as we can see in Figures 7a and 7b. The rapidity distributions presented in Figures 8a and 8b show that for $M_{Z'} = 1000$ GeV both models can not be clearly distinguished from each other in this case. If we consider $\sqrt{s} = 14$ TeV the rapidity distributions graphs are separated, mainly in the region $0 < y_{\mu\mu} < 1$, but this separation is not so noticeable as the one for $M_{Z'} = 1500$ GeV, already presented in Figures 3a and 3b. The transverse momentum distributions, presented in the Figures 9a and 9b, do not show a clear peak for $M_{Z'}/2$ for the Secluded model, but the Flipped one is put in evidence once again with higher values for this distribution on-peak. The muon angular distributions present a better behavior for disentangling both models, mainly if we consider $\sqrt{s} = 14$ TeV, as can be seen from Figures 10a and 10b.

4 Conclusions

In order to explore the properties of a new neutral vector boson belonging to models with $B - L$ local symmetry, we study the Drell-Yan channel with a muon pair production, for two LHC proposed scenarios: $\sqrt{s} = 7$ TeV ($\mathcal{L} = 1$ fb $^{-1}$) and $\sqrt{s} = 14$ TeV ($\mathcal{L} = 100$ fb $^{-1}$). Our study is focused on two values of the Z' boson mass, 1000 GeV and 1500 GeV.

First we can say that if $M_{Z'}$ is smaller than the centre of mass energy of the colliding protons, it can be discovered at the LHC. For instance, for $M_{Z'} = 1500$ GeV and $\sqrt{s} = 14$ TeV we obtain $\sim 10^8$ events for both $B - L$ models. The signals of Z' bosons come from their direct production.

In order to perform Z' studies in pp collisions, many observables can be used. We can cite the total cross-section and also several asymmetries very well studied by e^+e^- colliders. The measurement of some of these observables is very difficult due to the signal, which needs to be detected above the background of the hadronic experiment. Thus, it is necessary to apply cuts taking into account the detector acceptance for reducing the background contribution.

The invariant mass distribution of the muon pair final state is centered around the Z' mass. This behavior allows us to separate the signal from the background and to measure the Z' boson mass. Several cuts can be applied to guarantee more precision on measurements. The signal from the Flipped model is above the one from the Secluded model, and the corresponding difference can be enhanced if more severe cuts are considered. On the other hand, the SM background remains below the signals of both $B - L$ models, as shown in Figure 2.

The muon transverse momentum distribution centered around the half of Z' boson mass is a helpful observable for distinguishing the models. In this case we have observed a dominance of the Flipped model over the Secluded one, which has a behavior similar to the SM. See Figure 5.

The forward-backward charge asymmetry is another powerful tool to provide some information about the Z' couplings to quarks in pp collisions, when leptons are in the final state, even being measured indirectly due to the unknown of original quark direction. To guarantee the correct direction of the initial parton we applied a cut on final muon pair $|y_{\mu\mu}| > 0.8$. The resulting A_{FB} asymmetries, for both B-L models, present clear different behaviors, mainly for the muon pair invariant mass in the range 1300 – 1500 GeV, as shown in Figure 4.

In addition to A_{FB} , the rapidity distributions are very sensitive to the Z'

couplings to quarks and in their computing we can consider light and heavy quarks. They are very useful to disentangle the different models. Different cuts on it should be analyzed to exploit different responses from the same experiment. The combination of the forward-backward asymmetry and rapidity distribution generates another interesting observable, $A_{FB y_1}$. If the LHC discovers a Z' boson, the $A_{FB y_1}$ can be used as a refinement to select to which model the Z' boson belongs to. This combined observable is not under consideration in this work.

Besides the study for LHC operating in the high energy regime, we have performed an analysis at $\sqrt{s} = 7$ TeV for $M_{Z'} = 1000$ GeV. The obtained results present a clear signature for the Z' boson production. The dimuon invariant mass distribution shows a sharp peak around Z' boson mass, above the SM background, as shown in Figure 7. We note that the transverse momentum distribution once again reveals a peak on $p_T = M_{Z'}/2$. For these two distributions, the ones of the Flipped model are far above those of the Secluded model.

In general, the presented models can be well exploited by using the cited observables above at the LHC first energy stage. Some of them are more suitable for distinguishing the models. The choice of the applied cuts is also important. For instance, the same cuts that we had used to the forward-backward asymmetries are not appropriate to the rapidity distributions. Therefore, a combined analysis and different cuts should be applied to disentangle the models and guarantee more realistic theoretical prediction on the Z' couplings to fermions. The LHC running at $\sqrt{s} = 7$ TeV already is a powerful tool for unraveling physics beyond the SM.

Acknowledgements E. C. F. S. Fortes was supported by FAPESP under the process 07/59398-2; J. C. Montero was partially supported by CNPq under the process 307807/2006-1; Y. A. Coutinho thanks FAPERJ for financial support.

References

- [1] D. P. Barber *et al.*, Phys. Rev. Lett. **43**, 830 (1979).
- [2] G. Weiglein *et al.* (LHC/LC Study Group), Phys. Rept. **426**, 47 (2006).

- [3] R. W. Robinett and J. L. Rosner, Phys. Rev. D **25**, (1985) 3036; P. Langacker and M. Luo, *ibid.* D **45**, (1992) 278; J. Erler and P. Langacker, Phys. Rev. Lett. **84**, (2000) 212.
- [4] D. London and J. L. Rosner, Phys. Rev. D **34**, (1986) 1530; J. Kang and P. Langacker, Phys. Rev. D **71** (2005) 035014; P. Langacker, R. W. Robinett and J. L. Rosner, Phys. Rev. D **30**, 1470 (1984); J. L. Hewett, T. G. Rizzo, Phys. Rep. **183**, 193 (1989).
- [5] A. Davidson, Phys. Rev. D **20**, (1979) 776; V. Barger, E. Ma and K. Whisnant, Phys. Rev. D **26**, (1982) 2378; M. K. Parida and A. Raychaudhuri, Phys. Rev. D **26**, (1982) 2364.
- [6] N. Arkani-Hamed, A. G. Cohen and H. Georgi, Phys. Lett. B **513**, 232 (2001) ; N. Arkani-Hamed, A. G. Cohen, E. Katz and A. E. Nelson, JHEP **0207**, 034 (2002).
- [7] Vernon D. Barger, Wai-Yee Keung, Ernest Ma. Phys. Lett. B **94**, (1980) 377; Vernon D. Barger, Wai-Yee Keung, Ernest Ma. Phys. Rev. D **22** (1980) 727; Vernon D. Barger, Wai-Yee Keung, Ernest Ma. Phys. Rev. Lett. **44** (1980) 1169; H. Georgi and S. Weinberg, Phys. Rev. D **17** (1978) 275; E. H. De Groot, D. Schildknecht and G. J. Gounaris, University of Bielefeld Report No. BI-TP 79/37 (unpublished).
- [8] “Pedagogical Introduction to Extra Dimensions”, Thomas G. Rizzo, SLAC-PUB-10753, SSI-2004-L013, Sep 2004, arXiv:hep-ph/0409309v2.
- [9] F. Pisano and V. Pleitez, Phys. Rev. D **46**, 410 (1992).
- [10] P. H. Frampton, Phys. Rev. Lett. **69**, 2889 (1992).
- [11] J. E. Cieza Montalvo, M. D. Tonasse, Phys. Rev. D **67**, 075022 (2003).
- [12] De Curtis, Stefania, The BESS model revisited as a Higgsless Linear-Moose @ the LHC, arXiv:1002.2361.
- [13] T. Appelquist, B. A. Dobrescu, and A. R. Hopper, Phys. Rev. D **68**, 035012 (2003).
- [14] J. C. Montero and V. Pleitez, Phys. Lett. B **765**, 64 (2009).
- [15] E. C. F. S. Fortes, J. C. Montero, V. Pleitez, Phys. Rev. D **82**, 114007 (2010).
- [16] W. Emam, and S. Khalil, Eur. Phys. J. C **52**, 625 (2007).

- [17] A. Abulencia *et al.*, (CDF Collaboration), Phys. Rev. Lett. **96**, 211801 (2006); T. Aaltoni *et al.*, (CDF Collaboration), Phys. Rev. Lett. **102**, 091805 (2009).
- [18] J. Erler, P. Langacker, S. Munir, and E. Rojas, JHEP **08**, 017 (2009).
- [19] G. Cacciapaglia, C. Csáki, G. Marandella, and A. Strumia, Phys. Rev. D **74**, 033011 (2006).
- [20] E. Salvioni, G. Villadoro, and F. Zwirner, JHEP **11**, 068 (2009).x
- [21] K. Nakamura *et al.* (Particle Data Group), J. Phys. G **37**, 075021 (2010).
- [22] M. Boezio *et al.*, New J. Phys. **11**, 105023 (2009).
- [23] E. Boos *et al.*, [CompHEP Collaboration], CompHEP 4.4: Automatic computations from Lagrangians to events, Nucl. Instrum. Meth. A **534**, 250 (2004).
- [24] Michael Dittmar, Phys. Rev. D **55**, 161 (1997).
- [25] Michael Dittmar, Anne-Sylvie Nicollerat, Abdelhak Djouadi, Phys. Lett. B **583**, 111 (2004).
- [26] E. Ramirez Barreto, Y. A. Coutinho, J. Sá Borges, Phys. Lett. B. **689**, 36 (2010).

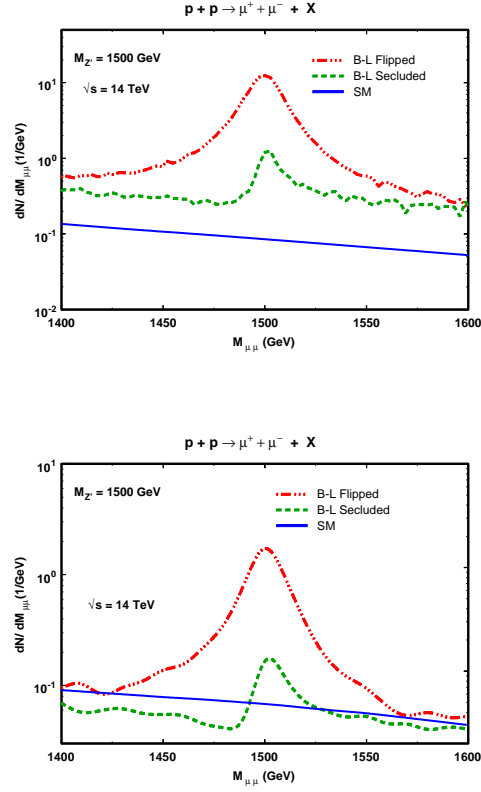


Figure 2: The dilepton invariant mass distribution for $p + p \rightarrow \mu^+ + \mu^- + X$ process for the Flipped, Secluded and Standard models considering $M_{Z'} = 1500$ GeV at $\sqrt{s} = 14$ TeV. First cut set (up) and second cut set (down).

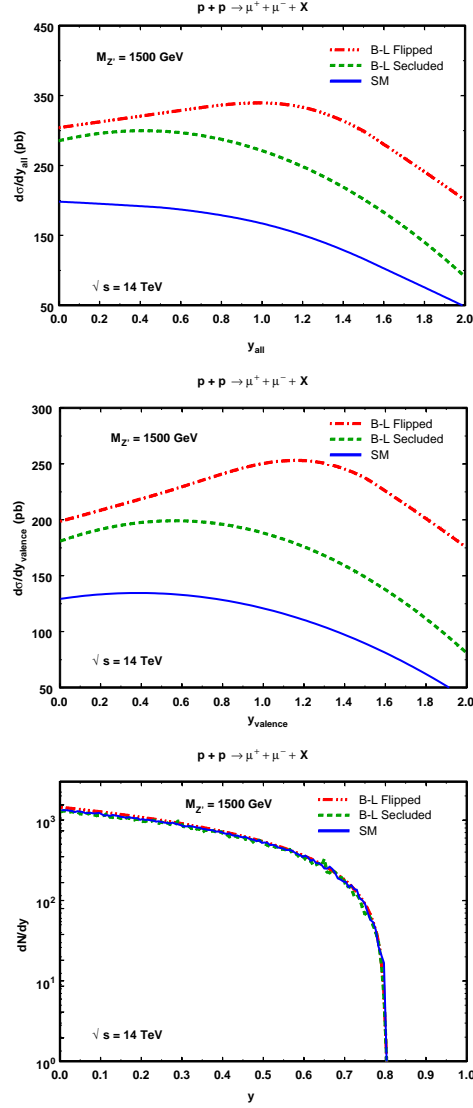


Figure 3: The rapidity distribution for the process $p + p \rightarrow \mu^+ + \mu^- + X$ considering $M_{Z'} = 1500$ GeV for the Flipped, Secluded and Standard models at $\sqrt{s} = 14$ TeV. The valence and sea quark contributions (up) and only the valence quarks (middle), using the first cut set. The same rapidity distribution using the second cut set (down).

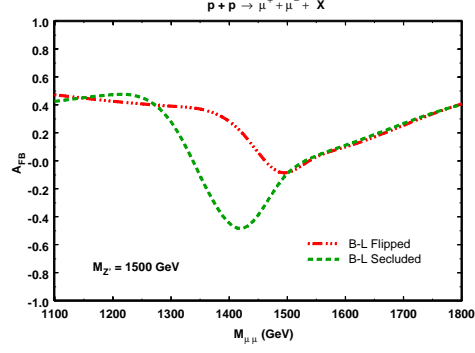


Figure 4: The forward-backward asymmetry for the process $p + p \rightarrow \mu^+ + \mu^- + X$ as a function of the dilepton invariant mass for both $B - L$ models, considering $M_{Z'} = 1500$ GeV, $\sqrt{s} = 14$ TeV, and applying the second cut set.

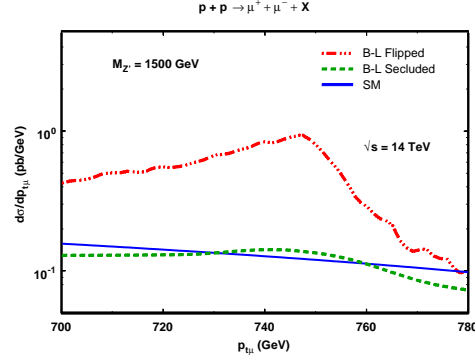


Figure 5: The muon transverse momentum distribution for the process $p + p \rightarrow \mu^+ + \mu^- + X$ for the Flipped, Secluded and Standard models, considering $M_{Z'} = 1500$ GeV, $\sqrt{s} = 14$ TeV, and applying the second cut set.

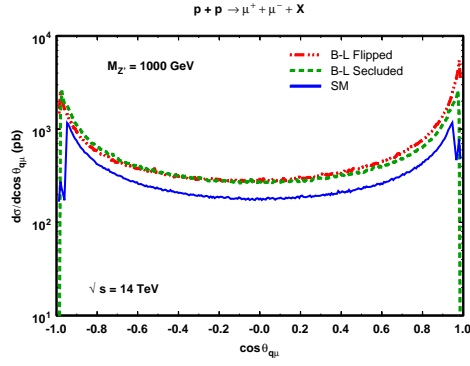


Figure 6: The muon angular distribution for the process $p+p \rightarrow \mu^+ + \mu^- + X$ for the Flipped, Secluded and Standard models, considering $M_{Z'} = 1000$ GeV and $\sqrt{s} = 14$ TeV.

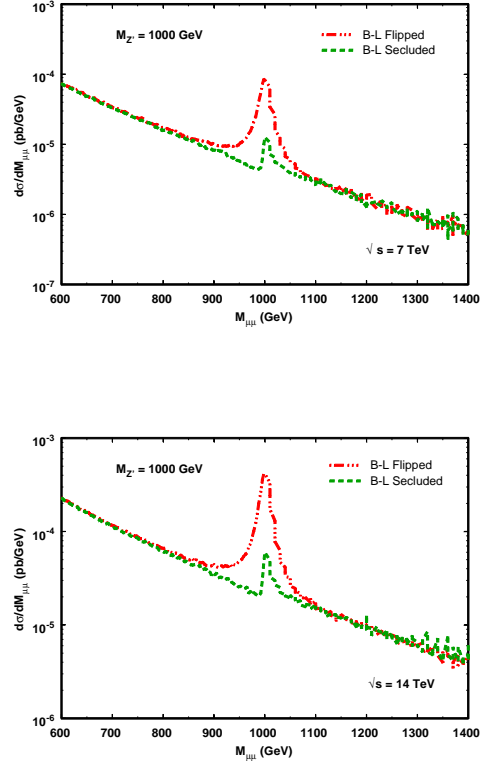


Figure 7: The dilepton invariant mass distribution for $p + p \rightarrow \mu^+ + \mu^- + X$ process in Flipped and Secluded models considering $M_{Z'} = 1000$ GeV at $\sqrt{s} = 7$ TeV (up) and $\sqrt{s} = 14$ TeV (down) with the first cuts set.

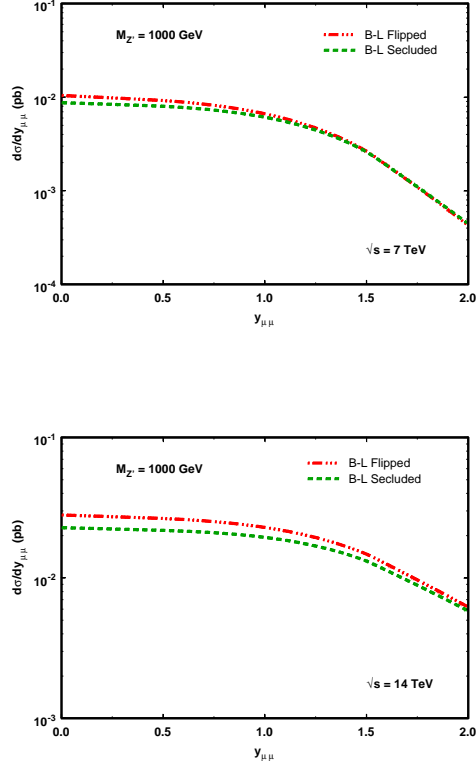


Figure 8: The rapidity distribution for the process $p + p \rightarrow \mu^+ + \mu^- + X$ for both $B - L$ models, considering $M_{Z'} = 1000 \text{ GeV}$, $\sqrt{s} = 7 \text{ TeV}$ (up) and $\sqrt{s} = 14 \text{ TeV}$ (down) with the first cut set.

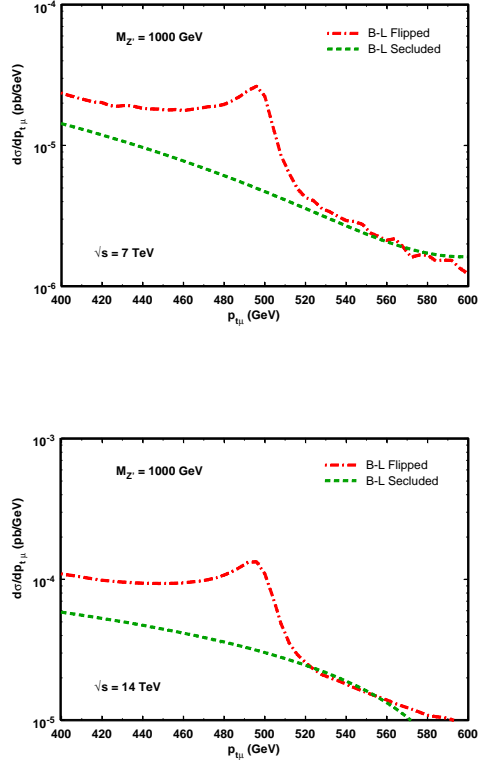


Figure 9: The muon transverse momentum distribution for the process $p + p \rightarrow \mu^+ + \mu^- + X$ for both $B - L$ models, considering $M_{Z'} = 1000$, $\sqrt{s} = 7$ TeV (up) and $\sqrt{s} = 14$ TeV (down), applying the first cut set.

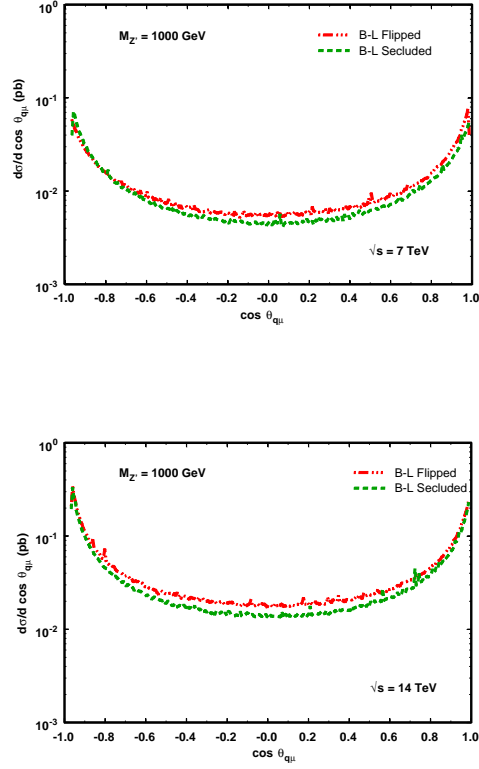


Figure 10: The muon angular distribution for the process $p + p \rightarrow \mu^+ + \mu^- + X$ for both $B - L$ models, considering $M_{Z'} = 1000$, $\sqrt{s} = 7$ TeV (up) and $\sqrt{s} = 14$ TeV (down), applying the first cut set.